Malaysian Journal of Analytical Sciences, Vol 21 No 4 (2017): 839 - 848
DOI: https://doi.org/10.17576/mjas-2017-2104-10

MALAYSIAN JOURNAL OF ANALYTICAL SCIENCES
Published by The Malaysian Analytical Sciences Society
ISSN 1394 - 2506

PRODUCTION OF ETHYLENE FROM ETHANOL DEHYDRATION OVER H_3PO_4-MODIFIED CERIUM OXIDE CATALYSTS

(Penghasilan Etilena Daripada Pendehidratan Etanol Dengan Mangkin Serium Oksida Terubahsuai H_3PO_4)

Soo Ling Chong[1], Jiah Chee Soh[1], Chin Kui Cheng[1,2]*

[1]*Faculty of Chemical & Natural Resources Engineering*
[2]*Centre of Excellence for Advanced Research in Fluid Flow*
Universiti Malaysia Pahang, 26300 Kuantan, Pahang, Malaysia

**Corresponding author: chinkui@ump.edu.my*

Received: 20 September 2016; Accepted: 16 May 2017

Abstract

Production of ethylene from ethanol dehydration was investigated over H_3PO_4 (10 wt.% to 30wt.%)-modified cerium oxide catalysts synthesized by wet impregnation technique. The prepared catalysts were characterized using scanning electron microscope (SEM), N_2 adsorption-desorption method, X-ray diffraction (XRD), Fourier transform infrared spectroscopy (FTIR) and thermogravimetric analysis (TGA) for the physicochemical properties. The ethanol catalytic dehydration was carried out in a fixed-bed reactor at 673-773 K and at ethanol partial pressure of 33 kPa. The effects of phosphorus loading on catalyst and reaction temperatures were investigated in terms of catalytic activity towards product selectivity and yield. Overall, the selectivity and yield of ethylene increased with the temperature and phosphorus loading. The highest ethylene selectivity and yield were 99% and 65%, respectively, at 773 K and 33 kPa over the 30 wt.% H_3PO_4-modified cerium oxide.

Keywords: ethylene production, ethanol dehydration, H_3PO_4 modification, cerium oxide

Abstrak

Penghasilan etilena daripada pendehidratan etanol telah dikaji dengan mangkin serium oksida terubahsuai H_3PO_4 (10 wt.% hingga 30 wt.%) yang dihasilkan melalui kaedah pengisitepuan. Mangkin disediakan telah dicirikan menggunakan mikroskop elektron imbasan (SEM), kaedah penjerapan-nyahjerapan N_2, pembelauan sinar-X (XRD), spektroskopi inframerah transformasi Fourier (FTIR) dan analisis termogravimetri (TGA) untuk mengetahui sifat fizikokimia mangkin. Tindak balas pendehidratan etanol dengan mangkin dilakukan di dalam reaktor turus terpadat pada julat suhu 673 – 773 K dan tekanan separa etanol 33 kPa. Pengaruh muatan H_3PO_4 dan suhu tindak balas kimia dalam pendehidratan etanol telah dikaji. Secara keseluruhan, kepilihan dan hasil etena meningkat dengan muatan H_3PO_4 dan suhu tindak balas kimia. Kepilihan dan hasil etena tertinggi masing-masing ialah 99% dan 65% pada 773 K dan 33kPa untuk mangkin serium oksida terubahsuai H_3PO_4 30 wt.%.

Kata kunci: penghasilan etilena, pendehidratan etanol, pengubahsuaian H_3PO_4, serium oksida

Introduction

The increasing demand of ethylene is due to its uses in producing polyethylene, one of the primary components in the most of the plastic and in petrochemical industry [1]. Besides that, ethylene acts as precursors for surfactant chemicals such as ethylene oxide or ethylene glycol. With increased demand, global ethylene production has grown at an average rate of almost 4.5% per year from 2009 – 2014. Currently steam cracking of hydrocarbon from fossil fuel is still dominating the production market because of the high production cost and energy consumption

associated with catalytic dehydration pathway. Due to the increasing demands for energy, stricter environmental regulations, and continued depletion of fossil feedstock, alternative and renewable energy resources have attracted increased interest in recent research. In the view of potential limitations of ethylene availability from the current sources, catalytic dehydration of ethanol (especially bioethanol) to ethylene has become a completely renewable process for producing ethylene [2].

Ethanol dehydration is a process in which water molecules are removed, or the equivalent of water molecules removed from ethanol to produce ethylene when heated together with catalyst. There are two reactions that occur in parallel during catalytic dehydration of ethanol as in Equation (1) to (2):

$$C_2H_5OH \leftrightarrow C_2H_4 + H_2O \qquad +44.9 \text{ kJ/mol} \qquad (1)$$

$$2C_2H_5OH \leftrightarrow C_2H_5OC_2H_5 + H_2O \qquad -25.1 \text{ kJ/mol} \qquad (2)$$

The low temperature favors the side reaction to produce diethyl ether; in contrast, higher reaction temperature is theoretically favoring the main reaction (ethanol dehydration). The dehydration reaction is endothermic and need 390 calories per gram of ethylene produced. The temperature of diethyl ether formation is mainly between 423 K and 573 K, while ethylene formation is favoured between 593 K and 773 K.

Acidic catalysts are often used in ethylene production from ethanol dehydration. The traditional homogeneous catalysts used are sulfuric acid or phosphoric acid in almost all industrial scale processes [1]. The former usually requires higher reaction temperatures and yields lower ethylene selectivity [3]. Due to the low yield and byproducts formation, sulfuric acid and phosphoric acid have been replaced by heterogeneous catalysts such as alumina.

Many studies have been carried out with different technologies and using various acidic heterogeneous catalysts such as alumina, silica, zeolites, metal oxides and heteropolyacids [4 - 7]. Among those studied catalysts, gamma alumina (γ-Al_2O_3) and HZSM-5 zeolite have drawn the most attention for their high activity and selectivity. HZSM-5 has been widely used in alcohol dehydration reactions due to its uniform pore structure, high surface area, and adjustable acidity. Low reaction temperature (>473 K) favors the reaction towards ethylene production from ethanol dehydration over HZSM-5. HZSM-5 can achieve 60 – 80% ethylene yield at relatively low reaction temperature (473 – 573 K) [8]. Besides of the reaction temperature, the catalyst surface acidity is a significant catalytic performance factor. HZSM-5 has high concentration of strong acidic sites, which exist at low Si/Al ratios helps in ethylene production. However, the high acidity also leads to render HZSM-5 zeolite unstable and low anti-coking property [9]. On the contrary, γ-Al_2O_3 has high surface area (50 –300 $m^2 g^{-1}$) and thermal stability up to 873 K that make it widely used in industrial. The ethanol dehydrate over γ-Al_2O_3 can achieve greater than 90% to form ethylene. The disadvantage of γ-Al_2O_3 is high reaction temperature needed for ethanol catalytic dehydration. Another problem is that water can deactivate active sites on γ-Al_2O_3 and inhibit the formation rate of ethylene and diethyl ether [10].

The weak acid centers and relatively strong acid centers of the catalyst are the active sites of ethanol intramolecular dehydration to ethylene [6]. However, the strong acid centers can easily lead to ethylene polymerization. Hence, surface acidity of catalyst need to adjust using additives to improve catalyst stability and high ethylene selectivity. In continuation of discovering new catalyst for ethanol catalytic dehydration, we report the use of ceria-based catalysts for the aforementioned reaction. The use of cerium oxide as the support bring advantages such as its high oxygen mobility associated with oxygen vacancies and oxygen storage capacity. Due to the high effectiveness of cerium oxide used as a support and the (phosphostic acid ad), many studies have been carried out by employing cerium oxide as catalyst for ethanol conversion reactions especially steam reforming reactions [11 - 15]. As mentioned earlier , the surface acidity of catalyst is improtant in this reaction. Thus, pure CeO_2 catalysts as well as phosphoric acid (H_3PO_4) doped CeO_2 catalysts were prepared to study the behavior of CeO_2 towards kinetics of ethanol dehydration.

Therefore, the aim of this study is to investigate the feasibility of ethanol dehydration over H_3PO_4-modified cerium oxide catalysts on new catalyst application for this reaction. The synthesized catalysts were characterized using

scanning electron microscope (SEM), energy dispersion X-ray spectroscopy (EDX), N_2 adsorption-desorption method, X-ray diffraction (XRD), Fourier transform infrared spectroscopy (FTIR) and thermogravimetric analysis (TGA) for the physicochemical properties.

Materials and Methods

Catalysts preparation

Cerium nitrate salt $Ce(NO_3)_2$ was procured from Sigma-Aldrich, USA. The ceria support was prepared by thermal decomposition of $Ce(NO_3)_2.6H_2O$ at 873 K for 2 hours and then crushed to powder. The modified cerium oxide phosphate catalyst (10PA-CeO_2) was prepared by impregnating the 10 wt.% aqueous solution of H_3PO_4 into 90 wt.% of the ceria support followed immediately by magnetic stirring for 3 hours. The solution was then magnetic-stirred for 3 hours under ambient condition. Thereafter, the impregnated catalyst was oven-dried for 12 hours at 373 K. During the first 6 hours of the drying process, the catalyst was manually stirred using a glass rod for each hour to maintain relative homogeneity of the slurry. Post 12 hours, the calcination of the dried catalyst was carried out in a muffled furnace model Carbolite RHF1400 for 5 hours at 773 K with heating rate of 5 K min^{-1}. The catalyst was then cooled to room temperature and ground for physicochemical characterization and reaction studies. The resulting 20PA-CeO_2 and 30PA-CeO_2 were prepared by the similar procedure with 20 wt.% and 30 wt.% of phosphoric acid, respectively.

Catalyst characterization

The fresh modified cerium oxide phosphate catalysts were characterized using several methods. The phase structure of the catalysts was characterized by X-ray diffraction (Rigaku Miniflex Instrument) using X-ray source from CuKα (λ=1.542 Å) at 30 kV and 15 mA. N_2 physisorption was conducted to determine the textural property of the synthesized catalysts. The information about the surface morphology of the catalyst and the elemental chemical compositions were determined using SEM analysis employing Hitachi TM3030Plus with a magnification of 5kx which was also equipped with energy-dispersive X-ray spectroscopy (EDX). Thermogravimetric-difference thermal analysis (TG) technique of samples before and after reaction was carried out to monitor the thermal profile of fresh and spent catalysts. Fourier Transform Infrared Spectroscopy (FTIR) (Perkin Elmer Spectrum 100) was also employed to determine the nature of chemical bonding of the catalysts.NH_3-TPD was carried out in a ThermoFinnigan TPDRO 1100. The catalyst was pre-treated with N_2 at 423 K for 15 minutes. NH_3-TPD is used to determine the amount of acidic sites and their distribution in strength. The adsorption of NH_3 was carried out at room temperature for 45 min and after saturation was achieved, N_2 was purged in to eliminate the NH_3 that remained in the gas phase. Analysis of desorption of NH_3 was done under the flow of helium at temperature of 323 to 1273 K, at the rate of 20 K min^{-1}.

Catalytic activity

The reaction was conducted in a fixed-bed reactor at ethanol partial pressure of 33 kPa with WHSV of 240 h^{-1}, in the temperature range of 673 – 773K. The reactor was loaded with 0.3 g of catalyst and introduced with pure ethanol (≥99.9%) with a HPLC pump. The gaseous products were collected and identified using GC to identify the quantity of targeted product. The GC instrument used was Shimadzu GC-2014 with two packed column, column temperature and flame ionizer detector temperature at 333 K and 473 K, respectively. Ethanol conversion and products selectivity were calculated by Equation (3) and (4), respectively [16, 17]:

$$X_{Ethanol} = \frac{\sum \text{Total gas products},F_i}{2 \text{ x molar flow rate of ethanol in the feed}} \text{ x } 100 \quad (3)$$

$$S_i = \frac{F_{C_2H_4}}{\Sigma \text{ Total gas products},F_i} \times 100 \quad (4)$$

where F is define as molar flow rate and *i* is refer to C_1, C_2, C_3, C_4 and C_5 species.

Results and Discussion

Catalyst characterization

Figure 1 illustrates XRD diffractogram of CeO_2 and 10, 20, 30PA-CeO_2. Based on Figure 1, the high intensity peaks recorded at 2θ readings of 28.6°, 33.1°, 47.48° and 56.36° which corresponding to (111), (200), (220) and

(311) crystal planes respectively.The XRD patterns obtained of the synthesized catalysts were compared with the standard data for CeO_2 (JCPDS card No. 34-0394).This also indicated that the CeO_2's structure maintained well for all modified catalysts [18]. The structure of catalysts became less crystalline as affected by H_3PO_4 loading. There are additional small peaks found for 20PA-CeO_2 and 30PA-CeO_2 at 2θ readings of 21°, 27° and 43° which can be ascribed to CeP_2O_7 species (JCPDS card No. 30-0164). CeP_2O_7 is a crystalline product in which every Ce atom is joined to six oxygen and every P to four oxygen, with a connectivity of four and six. The P atoms are joined in pairs through shared O atom to form $P_2O_7^{4-}$ units, each of it shared its six remaining oxygen with the CeO_6 octahedral. The appearance of CeP_2O_7 is normally occurred when cerium oxide reacted with phosphoric acid at temperature around 623 K to 1073 K. In this case, the modified cerium oxide phosphate catalysts were prepared at 773 K in a furnace which causes the formation of CeP_2O_7 species [19].

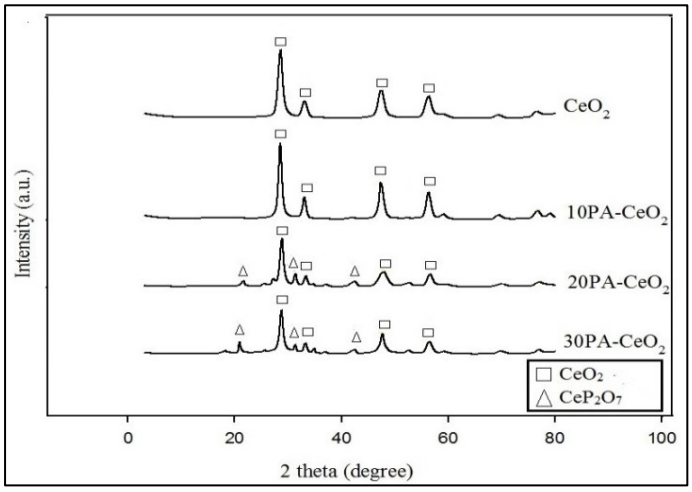

Figure 1. X-ray diffraction profiles of CeO_2 and H_3PO_4-modified CeO_2 catalysts

SEM micrographs of modified cerium oxide phosphate catalysts at 20 µm resolution are shown in Figure 2. Based on the Figure 2, most of the samples were agglomerated together. The SEM images shown in Figure 2 reveal the morphology of all samples is similar with formation of irregular and bulky surface which is typical of thermally-synthesized wet impregnated catalyst. Meanwhile, it is clearly proved that the addition of H_3PO_4 did not alter the surface morphology of the catalysts, and that the H_3PO_4 has blended intimately with the CeO_2 support to form a single phase.

The fresh catalysts were also subjected to the FTIR scanning and the spectra collected are shown in Figure 3. The spectra were recorded in the wave number that ranged 4000 – 400 cm^{-1}. Significantly, transmission band representing N-O stretch which normally can be found at wavenumber 3000 cm^{-1} is absent in Figure 3. This indicates that the entire nitrate group was successfully removed during the thermal decomposition of nitrate-salt to yield pure CeO_2. The transmission band at wave number 550.73 cm^{-1} represents the Ce-O stretch. In addition, the bands at wavenumber around 900 – 1000 cm^{-1} represent the O=P=O asymmetric stretching modes of phosphate or polyphosphate species[20]. As shown in Figure 3, the intense band found around 1000 – 1600 cm^{-1} increase as the loading of phosphorus increase. This is due to the introduction of phosphorus onto the CeO_2 catalyst whereby the O=P=O asymmetric increases. The same results observed in previous study [21]. This proves that introduction of H_3PO_4 has been successfully carried out.

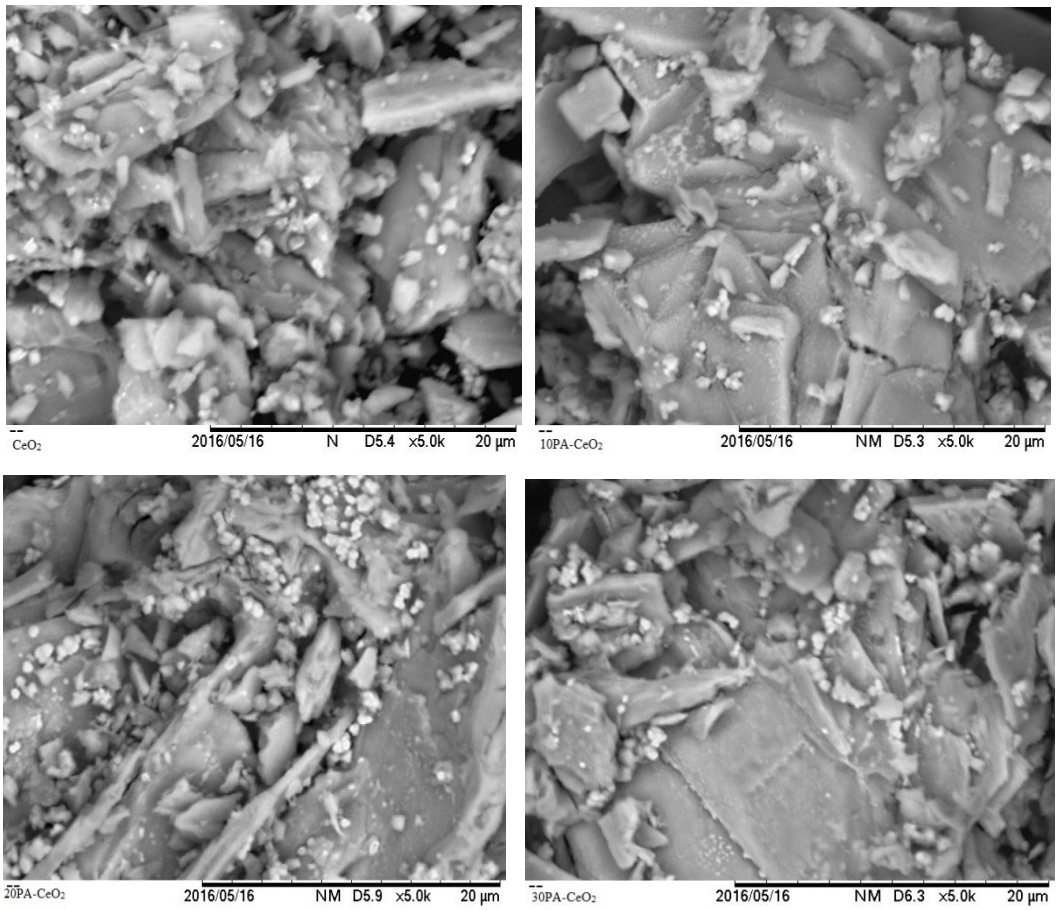

Figure 2. SEM images of CeO_2 and H_3PO_4-modified CeO_2 catalysts

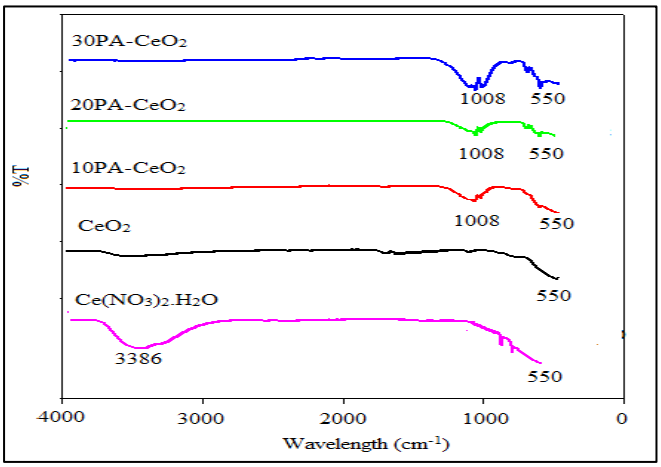

Figure 3. FTIR results of CeO_2 and H_3PO_4-modified CeO_2 catalysts

Table 1 provides the BET specific surface area, mesopore volume and pore diameter of pure CeO_2 and H_3PO_4-modified CeO_2 catalysts that were obtained from N_2 physisorption. Both the BET specific surface area and

mesopore volume decreased with H_3PO_4 loading, to the tune of nearly 90% reduction for the 30 wt.% H_3PO_4 loading. The reduction of pore dimension or pore blockage of the CeO_2 by the introducing of phosphoric acid in the treatment [22]. In contrast, the pore diameter recorded an increment, from 14.0 nm improved to 18.8 nm when the H_3PO_4 weight was increased. This could be due to the creation of wider pore mouth on the surface of CeO_2 resulting from the acid attack that occurred at the employed calcination temperature.

Table 1. Textural properties of the CeO_2 and H_3PO_4-modified CeO_2 catalysts

Fresh Catalyst	BET Specific Surface Area ($m^2\ g^{-1}$)	Pore Volume ($cm^3\ g^{-1}$)	Pore Diameter (nm)
CeO_2	71.6	0.2545	14.0
10PA-CeO_2	35.5	0.1461	16.3
20PA-CeO_2	20.2	0.0833	16.3
30PA-CeO_2	9.9	0.0461	18.8

Thermo-desorption profiles of NH_3 were carried out to determine the acid-base properties of the as-synthesized catalysts. The acid strength can be categorized into weak acidic site (373-523 K), moderate acidic site (523-673 K) and strong acidic site (673- 823 K), respectively, based on the desorption temperature. Table 2 shows the resulting acid amount of CeO_2 and H_3PO_4-modified CeO_2 catalysts. From Table 2, it can be observed that there are three types of acid sites with variable amounts, at 819 μmol g^{-1}, 188 μmol g^{-1} and 548 μmol g^{-1}, respectively, for weak, moderate and strong acids found in CeO_2 catalyst. The introduction of H_3PO_4 generates moderate acid sites by suppressing the strong acid sites of CeO_2. The amount of moderately-strong acid site has increased substantially, increasing incrementally to 837 μmol g^{-1} for 10PA- CeO_2, 1238 μmol g^{-1} for 20PA- CeO_2 and 1532 μmol g^{-1} for 30PA- CeO_2, respectively. This may be due to the nature of H_3PO_4, which is a moderately-strong acid with pKa value of 6.9 x 10^{-3}. Moreover, the strong acid site which was inititally present on the surface of pure CeO_2 was dimishing with the H_3PO_4 loading, decreased from 548 μmol g^{-1} for pure CeO_2 to just 284 μmol g^{-1} for 30PA-CeO_2 catalyst. As the loading of phosphoric acid on CeO_2 increases, the total acid amount increases.

Table 2. The total surface acidity and acid strength distribution of CeO_2 and H_3PO_4-modified CeO_2 catalysts

Catalysts	Acid Amount (μmol g^{-1})			Total Acid Amount (μmol g^{-1})
	Weak Acid Site (373-523 K)	Moderate Acid Site (523-673 K)	Strong Acid Site (673-823 K)	
CeO_2	819	188	548	1555
10PA-CeO_2	850	837	413	2100
20PA-CeO_2	838	1238	385	2461
30PA-CeO_2	823	1532	284	2639

Catalytic performances of modified cerium oxide phosphate catalysts

Table 3 shows the product distribution over CeO_2 and 10, 20, 30PA- CeO_2 catalyst at different reaction temperature and ethanol partial pressure 33 kPa. Cerium oxide catalyst presented lowest catalytic performance among all synthesized catalysts. The pure CeO_2 catalyst, under the same reaction condition as aforementioned, the conversions recorded were 1.25%, 2.45% and 6.89%, respectively. This reveals that the acidity amount found in CeO_2cannot protonate the hydroxyl group of C_2H_5OH which explains its low activity. The selectivity decreases with the increasing reaction temperature. This is due to higher hydrocarbons formation with almost 35% at 773 K. CeO_2 presents highest number of strong acidic sites which lead to the higher hydrocarbons formation [16], [22]. Hence, there were over 45% of hydrocarbons formed over CeO_2 catalyst at high temperature.

Table 3. Product distributions of ethanol dehydration over CeO_2 and H_3PO_4-modified CeO_2 catalysts at 33 kPa and 673 – 773 K

Variable	CeO_2			10PA-CeO_2			20PA-CeO_2			30PA-CeO_2		
	Temperature (K)			Temperature (K)			Temperature (K)			Temperature (K)		
	673	723	773	673	723	773	673	723	773	673	723	773
Ethanol conversion (%)	1.23	2.45	6.89	4.79	8.96	29.90	9.39	35.73	41.31	15.97	38.02	59.74
Selectivity (%)												
Ethylene	68.71	53.76	47.20	47.2	54.60	70.39	94.11	95.35	98.33	96.14	98.55	99.21
Higher hydrocarbons												
C_3	0.28	0.81	3.25	0.01	1.18	0.28	0	0.01	0.01	0	0.01	0.01
C_4	7.73	21.13	22.93	0.14	6.32	2.17	0.2	0.14	0.11	0.2	0.11	0.14
C_5	19.78	0	8.01	0.44	4.01	3.78	3.30	0.44	1.12	3.30	1.12	0.44
C_6	0	14.90	0.10	0	0	0.14	0	0	0	0	0	0

The ethanol conversion, ethylene selectivity and total acid amountwere correlated for the synthesized catalysts in Figure 4. Upon doing with H_3PO_4, the ethylene selectivity and ethanol conversion increase as the loading of H_3PO_4 increase. The addition of H_3PO_4 into CeO_2 catalyst causes the amount of strong acidic sites decrease. This change suppresses the formation of higher hydrocarbons and improves the ethylene production. Although 10PA-CeO_2 did not present a high catalytic performance with low ethanol conversion 4.79%, 8.96% and 29.90% for 673 K, 723 K and 773 K, respectively, but it showed increasing trend in terms of catalytic performance as compared to pure CeO_2. This indicates that the surface acidity of 10PA-CeO_2 was unable to catalyze the formation of products. Among all CeO_2 and H_3PO_4-modified CeO_2 catalysts, the 30PA-CeO_2 catalyst showed the best catalytic performance. On this catalyst, the products are dominated by ethylene under all reaction condition with over 95% of ethylene selectivity.

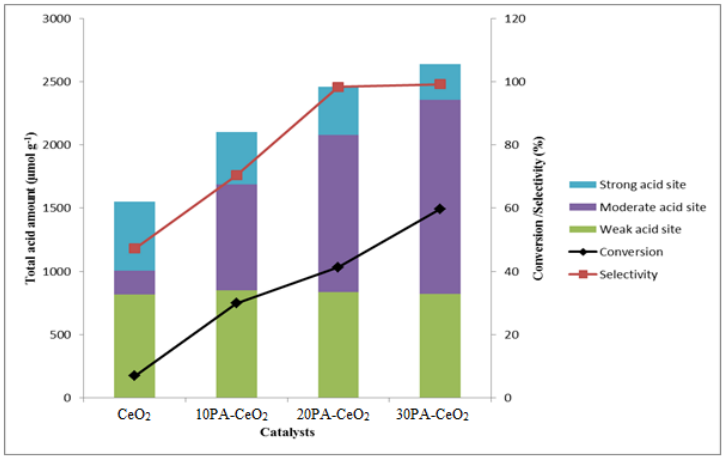

Figure 4. Relationship between catalytic performances and acid amounts

The presence of moderate weak acidic sites in this catalyst helps to suppress the formation of higher hydrocarbons meanwhile improved the ethylene production and selectivity. Besides that, based on the N_2 physisorption results CeO_2 has a large BET surface area and high porosity which lead to the C_2H_5OH molecules would have voyage

profound into the arrangement of passage systems that exists in the pristine CeO_2. The blockage of pore volume after the addition of H_3PO_4 helps in reducing the multiple adsorptions of ethanol whereby results in the improvement in ethylene selectivity [22].

In addition, 10, 20 and 30PA-CeO_2 present an increasing trend in both ethanol conversion and ethylene selectivity as the temperature increases. Among all the CeO_2 and H_3PO_4-modified CeO_2 catalysts, 30PA-CeO_2 catalyst showed the best catalytic performance. With increasing reaction temperature, both ethanol conversion and ethylene selectivity increased, *viz*. conversion of ethanol increased from 15.97% at 673 K to 59.74% at 773 K, whilst the ethylene selectivity improved from a low of 96.14% at 673 K to 99% at 773 K. This showed that the dehydration activity of 30PA-CeO_2 catalyst improved with reaction temperature. This indicates that H_3PO_4 functioned more effectively with reaction temperature, *i.e*. its acidity property can be tailored to the reaction temperature and thus, able to protonate the hydroxyl group of C_2H_5OH molecule.

Post reaction study

Among all CeO_2 and H_3PO_4-modified CeO_2 catalysts, 30PA-CeO_2 catalysts showed the best catalytic performance. The 30PA-CeO_2 catalyst was collected for post reaction characterization. The used 30PA-CeO_2catalysts at different reaction temperatures (673 K, 723 K and 773 K) were collected and were subjected to further examinations. Figure 5 shows the SEM image of the post-reaction 30PA-CeO_2 catalysts. It can be visualized that there are not much changes to the catalysts' morphology. In addition, no visible carbon formation was found after the reaction. This result suggests that the addition of 30wt% phosphoric acid enhance the stability of catalysis by weakening the strong acidic sites into moderate weak acidic sites. This prevent the double bond which is π bond found in C_2H_4 is electron rich from being attracted toward the acidic catalyst surface and form single C-C bond which lead to coke formation [23].

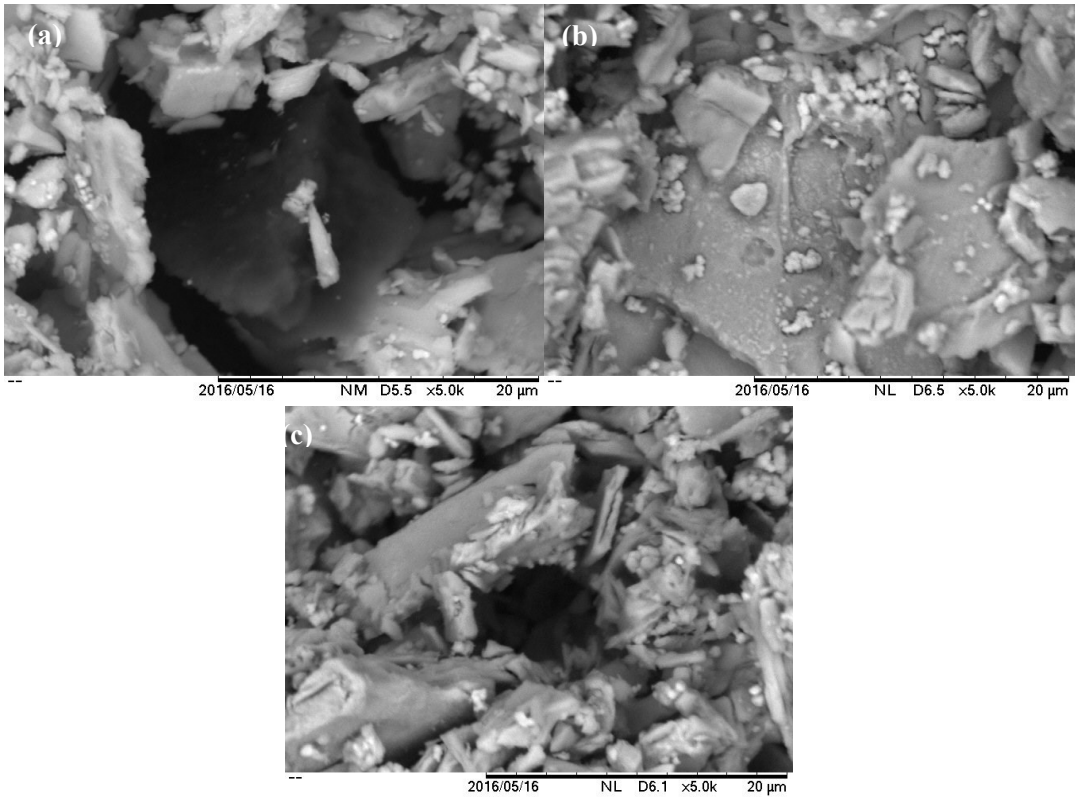

Figure 5. SEM images of 30PA-CeO_2 catalysts at ethanol partial pressure 33 kPa and (a) 673 K (b) 723 K and (c) 773 K.

TG analysis was performed to study the thermal profile of the spent 30PA-CeO_2 catalysts. The TG analysis was performed from 298 K to 1173 K, each time. As shown in Figure 6, weight loss in the used catalyst at all reaction temperatures are small. Indeed, the total weight loss of used 30PA-CeO_2 at reaction temperature 673 K was about 0.84 wt.%. For the used 30PA-CeO_2 catalyst at reaction temperatures of 723 K and 773 K, the weight losses at 873 K and 1073 K were 0.86 wt.% and 0.915 wt.%, respectively. This weight loss can be ascribed to the loss of water in catalyst and was consistent with the SEM results where no visible carbon formation was found. The results obtained also indicate that 30PA-CeO_2 catalyst was thermally stable.

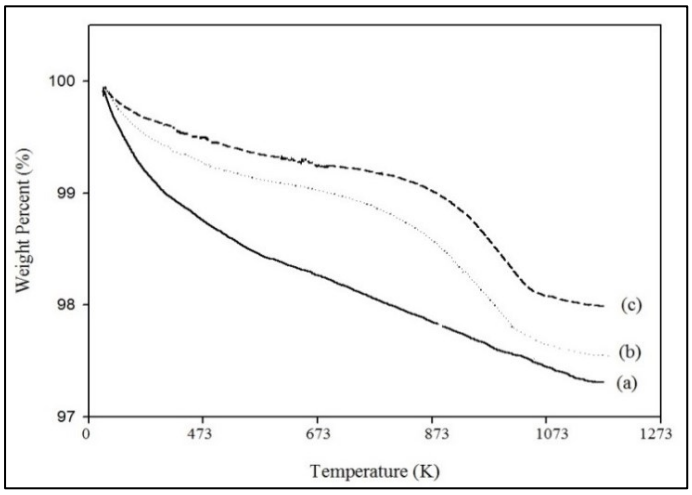

Figure 6. TGA profiles of used 30PA- CeO_2 catalysts at (a) 673 K, (b) 723 K and (c) 773 K

Conclusion

This project focuses on the catalytic performance of ethanol to ethylene on H_3PO_4-modified CeO_2 (various loadings of H_3PO_4) catalysts and the influences of H_3PO_4 on ethanol conversion over the synthesized catalysts. The addition of phosphorus acid to the CeO_2 catalyst improved the catalytic performance and catalyst stability for ethanol dehydration to ethylene. These improvements are due to the tuned acid sites and reduction of BET specific surface areaby preventing coke formation and blocking the accessibility of reactants to the acid sites.The H_3PO_4-modified CeO_2 catalysts showed increasing trend in ethanol conversion and ethylene selectivity with the loading of phosphorus. The post reaction analyses on the 30PA-CeO_2 catalyst (the best performing catalyst) also showed that the introduction of H_3PO_4 acid has helped in maintaining coke-free surface that would have otherwise caused catalyst deactivation. This can be attributed to the mild acidity sites available on the 30PA-CeO_2 catalyst.

Acknowledgement

We thank Universiti Malaysia Pahang for providing UMP Short Term Grant RDU160335 to support this work.

References

1. Morschbacker, A. (2009). Bio-ethanol based ethylene.*Polymer Review*, 49 :79 – 84.
2. Takahara, I., Saito, M., Inaba, M. and Murata, K. (2005). Dehydration of ethanol into ethylene over solid acid catalysts.*Catalysis Letters*, 10(3–4): 249 – 252.
3. Fan, D., Dai, D.-J., and Wu, H.-S. (2012). Ethylene formation by catalytic dehydration of ethanol with industrial considerations. *Materials (Basel)*, 6(1): 101 – 115.
4. Aguayo, A. T., Gayubo, A. G., Atutxa, A., Valle, B. and Bilbao, J. (2015). Regeneration of a HZSM-5 zeolite catalyst deactivated in the transformation of aqueous ethanol into hydrocarbons. *Catalysis Today*, 107 – 108: 410 – 416.

5. Phung, T. K., Radikapratama, R., Garbarino, G., Lagazzo, A., Riani, P. and Busca, G. (2015). Tuning of product selectivity in the conversion of ethanol to hydrocarbons over H-ZSM-5 based zeolite catalysts. *Fuel Processing Technology*, 137: 290 – 297.
6. Phung,T. K., Proietti Hernández, L.,Lagazzo, A. and Busca, G. (2015). Dehydration of ethanol over zeolites, silica alumina and alumina: Lewis acidity, Brønsted acidity and confinement effects. *Applied Catalysis A General*, 493: 77 – 89.
7. Varisli, D., Dogu, T. and Dogu, G. (2007). Ethylene and diethyl-ether production by dehydration reaction of ethanol over different heteropolyacid catalysts. *Chemical Engineering Science*, 62: 5349 – 5352.
8. Madeira, F. F., Gnep, N. S., Magnoux, P., Maury, S. and Cadran, N. (2009). Ethanol transformation over HFAU, HBEA and HMFI zeolites presenting similar Brønsted acidity. *Applied Catalysis A General*, 367(1–2): 39 – 46.
9. Zhan, N., Hu, Y., Li, H., Yu, D., Han, Y. and Huang, H. (2010). Lanthanum-phosphorous modified HZSM-5 catalysts in dehydration of ethanol to ethylene: A comparative analysis. *Catalysis Communications*, 11(7): 633 – 637.
10. DeWilde, J. F., Chiang, H., Hickman, D., Ho, C. R., and Bhan, A. (2013). Kinetics and mechanism of ethanol dehydration on γ-Al_2O_3: Tthe critical role of dimer inibition. *ACS Catalysis*, 3(4): 798 – 807.
11. Cai, W., Wang, F.,Zhan, E.,Van Veen, A. C., Mirodatos, C. and Shen,W. (2008). Hydrogen production from ethanol over Ir/CeO_2 catalysts: A comparative study of steam reforming, partial oxidation and oxidative steam reforming. *Journal of Catalysis*, 257(1): 96 – 107.
12. Diagne, C., Idriss, H. and Kiennemann, A. (2002). Hydrogen production by ethanol reforming over Rh/CeO_2–ZrO_2 catalysts. *Catalysis Communications*, 3(12): 565 – 571.
13. Mudiyanselage, K., Al-Shankiti, I., Foulis, A., Llorca, J. and Idriss, H. (2016). Reactions of ethanol over CeO_2 and Ru/CeO_2 catalysts. *Applied Catalysis B Environmental*, 197: 198 - 205.
14. Wang, H., Ye, J., Liu, Y., Li, Y. and Qin, Y. (2007). Steam reforming of ethanol over Co_3O_4/CeO_2 catalysts prepared by different methods. *Catalysis Today*, 129(3–4): 305 – 312.
15. Zhang, B., Tang, X., Li, Y., Cai, W., Xu, Y. and Shen, W. (2006). Steam reforming of bio-ethanol for the production of hydrogen over ceria-supported Co, Ir and Ni catalysts. *Catalysis Communications*, 7(6): 367–372.
16. Ramesh, K., Jie, C., Han, Y. F. and Borgna, A. (2010). Synthesis, characterization, and catalytic activity of phosphorus modified H-ZSM-5 catalysts in selective ethanol dehydration. *Industrial Engineering Chemistry Research*, 49(9): 4080 – 4090.
17. Zhang, X., Wang, R., Yang, X. and Zhang, F. (2008). Comparison of four catalysts in the catalytic dehydration of ethanol to ethylene. *Microporous Mesoporous Materials*, 116(1–3): 210 – 215.
18. Yacob, A. R., Bello, A. M. and Kabo, K. S. (2016). The effect of polyoxyethylene (40) stearate surfactant on novel synthesis of mesoporous γ-alumina from Kano kaolin. *Arabian Jounal of Chemistry*, 9(2): 297 –3 04.
19. White, K. M., Lee, P. L., Chupas, P. J., Chapman, K. W., Payzant, E. A., Jupe, A. C., Bassett, W. A., Zha, C. S. and Wilkinson, A. P. (2008). Synthesis, symmetry, and physical properties of cerium pyrophosphate. *Chemistry of Materials*, 20(11): 3728 – 3734.
20. Armaroli, T., Busca, G., Carlini, C., Giuttari, M., Raspolli Galletti, A. M. and Sbrana, G. (2000). Acid sites characterization of niobium phosphate catalysts and their activity in fructose dehydration to 5-hydroxymethyl-2-furaldehyde. *Journal of Molecular Catalysis A Chemical*, 151(1): 233 – 243.
21. Brandão, R. F., Quirino, R. L., Mello,V. M., Tavares, A. P., Peres, A. C.,Guinhos, F., Rubim, J. C. and Suarez, P. A. Z. (2009). Synthesis, characterization and use of Nb_2O_5 based catalysts in producing biofuels by transesterification, esterification and pyrolysis. *Journal of the Brazilian Chemical Society*, 20(5): 954 – 966.
22. Ramesh,K., Hui, L. M., Han,Y. F., and Borgna, A. (2009). Structure and reactivity of phosphorous modified H-ZSM-5 catalysts for ethanol dehydration. *Catalysis Communications*, 10(5): 567 – 571.
23. Zaera, F. (2001). Probing catalytic reactions at surfaces. *Progress Surface Science*, 69(1):1 – 98.